# Mechanical properties and behaviour of in-situ materials which are stabilised with bitumen emulsion

I. Pérez[1a]; L. Medina[a]; M. A. del Val[b]
[a] *Universidade da Coruña,, E. T. S. I. Caminos, Campus de Elviña, 15071 A Coruña, Spain*
[b] *Technical University of Madrid - UPM, Department of Civil Engineering-Transport, Ciudad Universitaria, 28040 Madrid, Spain*

**Abstract**

This paper presents a critical review of the mechanical properties of the materials used in the structural design of in-situ materials which are stabilised with bitumen emulsion. A description is provided of the types of materials that are stabilised with bitumen emulsion presently available and different hypotheses about their behaviour and different properties are put forth. The two main categories of mechanical properties investigated in the laboratory by means of mechanical test are addressed: a) properties similar to those of granular materials in accordance with their stress dependent behaviour; b) properties resembling hot mix asphalt materials in accordance with their temperature and time dependent viscoelastic behaviour. The article concludes with several final remarks on the structural behaviour and mechanical properties of these materials.

**Keywords**: rehabilitation, recycled materials, bitumen emulsion, mechanical properties

## 1. Introduction

A technique of unquestionable interest in pavement rehabilitation is cold in-situ stabilisation with bitumen emulsion of the old layers of the pavement. Some of the most important advantages are the savings on the consumption of aggregates and the better use made of aging binders. These savings also result in the reduction of the environmental impact caused by aggregate extraction and the emission of greenhouse gases released during the binder heating process. In addition, cold in-situ stabilisation does not produce hazardous emissions that can cause cancer in pavement rehabilitation workers. Another advantage is that since no heating is involved, there is no degradation of the aging binder or the binder used in the form of emulsion.

In recent years research on materials which are stalilised with bitumen emulsion (BSM**)** has been mainly aimed at characterization, formulation and implementation. Significant process has been made in the afore-mentioned fields. However, not as much research has been done in terms of acquiring

[1] Corresponding author. Tel: (+34) 981.167.000-Ext. 1451. Fax: (+34) 981.167.170. E-mail:iperez@udc.es

knowledge on the mechanical behaviour of these materials in order to improve the structural design of BSM. This article aims to review the mechanical properties and parameters used in the structural design of BSM.

**2. Types of BSM**

First, it is necessary to present the terms that are used in the scientific literature to describe BSM techniques. The reason for this is that the sections below will mention these terms when describing the properties and mechanical parameters. In South Africa, Ebels (2008) defines BSM as an action on the rehabilitation of pavements that typically consists of the following operations: the existing pavement is milled to a depth of 300 mm; it is treated with bitumen emulsion or foamed asphalt often in conjunction with the addition of a small percentage of active filler; water and compaction of the mixture. According to Ebels, in South Africa BSM are used to rehabilitate both the bituminous part of the pavement (Reclaimed Asphalt Pavement, RAP), and all or part of the base layer that is either granular or stabilised with cement. In keeping with this, in the USA two main BSM techniques can be distinguished (May, 2008; Cross & Jakatimath, 2007):

- Cold in-place Recycling (CIR) is a surface recycling technique in which the upper part of the bituminous pavement is milled and mixed with stabilising agents (bitumen emulsion or foamed asphalt) giving rise to a stabilised base course. The layer is stabilised with 100% RAP, with a thickness ranging from 75 to 100 mm.
- Full Depth Reclamation (FDR) is a reclamation technique in which the complete layer of the bituminous pavement and a specified thickness of a granular or cement-treated base course are crushed, pulverized and blended, giving rise to a base course stabilised with bitumen emulsion or foamed asphalt. The layer is not stabilised with 100% RAP and its thickness ranges between 100 and 300 mm.

**3. Behavioural phases of BSM**

Before studying the mechanical properties and parameters governing the mechanical behaviour of BSM, it is opportune to review the hypotheses related to this behaviour. In the technical bibliography consulted, two different hypotheses were generally found. They were each made up of two clearly

defined stages, but of a different nature. The first hypothesis assumed the following two phases (Liebenberg & Visser, 2003; 2004) (Figure 1a):

1. Effective Fatigue Phase: In principle, after the execution of the BSM, the material takes on a stiffness similar to that of a material that has been slightly improved with cement. This stiffness gradually diminishes, causing the material to fail due to fatigue.
2. Equivalent Granular Phase: The stiffness of the cracked material is similar to that of an unbound granular material. The material will fail due to reduced resistance to permanent deformation.

It is assumed that the fatigue life of BSM is used up when the final elastic modulus of the material is 500 MPa. This value represents approximately 25% of the initial stiffness of the material. For the purpose of analyzing fatigue, the critical parameter, which indicated the material´s flexibility, is the Strain-at-break. After fatigue, the behaviour is similar to that of unbound granular materials, although with a greater stiffness modulus. In this case, the failure is due to the shear stress and the critical mechanism is the resistance to permanent deformation. This two-phase approach is based on the structural design of cement-treated materials in South Africa and on full-scale test results using a Heavy Vehicle Simulator (HVS) (Theyse et al., 1996). In this manner, Liebenberg & Visser (2003; 2004) adjusted laws that predict the number of load repetitions ($N_f$) during the "Effective Fatigue Phase", in addition to other laws that predict the number of load repetitions ($N_{PD}$) during the "Equivalent Granular Phase". The total service life of the BSM layer is equal to $N_f + N_{PD}$. The full-scale tests were carried out on BSM sections with low RAP content (the original section consisting of surface treatment, base course stabilised with cement and granular subbase). The final section was made up of bituminous pavement (40 mm), BSM base with 1.8% residual bitumen and 2% cement (250 mm) and granular subbase (150 mm).

According to Jenkins et al. (2007) the observation of Long-Term Pavement Performance (**LTPP**) indicates that during the first phase of life the stiffness of BSM layers does not decrease; rather it increases due to the curing of the mixture. In keeping with this, several investigators (Loizos & Papavasiliou, 2006; Kumar et al., 2008) have used the Falling Weight Deflectometer (**FWD**) to evaluate the structural capacity of pavements rehabilitated by means of BSM techniques. They found

a substantial improvement in the stiffness of the BSM layer after some time, without any evidence of either the "Effective Fatigue Phase" or the **"**Equivalent Granular Phase". In the opinion of Ebels (2008), the idea behind Figure 1a is erroneous because in BSM fatigue only occurs after substantial time and most of the permanent deformation takes place in the pavement's early life. For all of the above reasons, Ebels (2008) proposes a more reliable second hypothesis based on in-place gathered data, consisting of two phases as well. (Figure 1b):

Comentario [MS1]: "Con el tiempo"

1. Curing Phase: An increase in the initial stiffness occurs due to the moisture reduction and densification in the BSM layer. This first phase may last between 6 and 18 months.
2. Stiffness Reduction Phase: A decrease in the stiffness of BSM layer occurs.

In accordance with Ebels (2008), Thomas & May (2007) and Jenkins & Yu (2009), these materials play an important structural role which falls within the range of the application of the granular materials and Hot Mix Asphalt (HMA) materials (Figure 2). In this role, the bitumen and cement content have primordial importance. In general, an increase in the bitumen content results in increased moisture resistance and flexibility, while an increase in cement content results in increased permanent deformation resistance and reduced flexibility (Figure 2).

According to Ebels (2008) and Jenkins & Yu (2009), in the first phase, the BSM is not equivalent to a material slightly improved with cement; instead it resembles an unbound granular material with stress dependent behaviour, whose properties have been improved by the addition of a bitumen emulsion. In this case, the most important property should be the resistance to shear stress. In the second phase, however, although the material is not comparable to HMA, it shows a tendency towards viscoelastic behaviour with some temperature and time dependent behaviour. But cracking due to fatigue should not be the dominant failure criterion. According to Santagata et al. (2010) stiffness is usually quite limited in the short term. This could lead to serious problems with the road, both during the construction of the pavement when the road building machinery might overload the BSM layer and immediately after it has been opened to traffic. In these conditions, significant permanent deformation may occur and failure conditions may be reached creating an irreversibly negative effect on the structural and functional state of the pavement. For this reason, Loizos & Papavasiliou (2006)

stated that prior to the curing of BSM; a HMA layer must be extended on top. However, based on our experience in Spain, it is considered necessary to wait until the moisture has completely evaporated before extending a layer on top (del Val, 1998).

## 4. Mechanical properties of BSM

In accordance with a review of the technical literature, it is possible to group the mechanical properties of BSM into two categories: properties of the unbound granular materials in accordance with their stress dependent behaviour, and properties of HMA in accordance with their temperature and time dependent viscoelastic behaviour.

### 4.1. *Properties of unbound granular materials*

4.1.1. *Permanent deformation*

In keeping with Jenkins et al. (2007), in BSM the cohesion ($c$) and the angle of internal friction ($\phi$) (estimated from the Möhr-Coulomb failure line created on the basis of static triaxial test results), determine the resistance to shear stress, and therefore, their resistance to permanent deformation. Good compaction (greater density) results in an increase in both parameters and consequently reduces the risk of shear failure. It is important that the BSM layers (especially those with low bitumen content) not be subjected to a large amount of moisture for a long period of time, since this would have a negative effect on their resistance to shear stress (Jenkins et al. 2007).

According to Jenkins et al. (2007) an increase in the content of bitumen results in a decrease of $\phi$. Ebels (2008) observed that in materials containing 25% RAP, for constant bitumen content, the addition of 1% cement produced an increase in $c$ and a decrease in $\phi$. The increase of the RAP percentage from 25 to 75% produced an increase in $c$ and a decrease in $\phi$ (Table 1).

On the other hand, for BSM there are very few predictive approaches of accumulated permanent deformation. Ebels (2008) conducted triaxial dynamic tests to obtain the cumulative permanent strain ($\varepsilon_p$) versus the number of load cycles (N). He then adjusted a double exponential model that predicts the three phases of the cumulative permanent strain:

$$\varepsilon_p = A\left(\frac{N}{1000}\right)^B + C\left(e^{D\frac{N}{1000}} - 1\right) \quad \textbf{(1)}$$

$$A = a_1(SR)^{a_2}\ ;\ B = b_1(SR)^{b_2}\ ;\ C = c_1(SR)^{c_2}\ ;\ D = d_1(SR)^{d_2}$$

where $a_1$, $a_2$, $b_1$, $b_2$, $c_1$, $c_2$, $d_1$, $d_2$=coefficients. SR refers to the Stress Ratio, which is expressed as the quotient between the deviator stress ($\sigma_d$) and the deviator stress at failure ($\sigma_{d,f}$) on a Möhr-Coulomb line (Liebenberg & Visser, 2003):

$$SR = \frac{\sigma_d}{\sigma_{d,f}} = \frac{\sigma_1 - \sigma_3}{\sigma_3\left[\tan^2\left(45^o + \frac{\phi}{2}\right) - 1\right] + 2c\tan\left(45^o + \frac{\phi}{2}\right)} \quad \textbf{(2)}$$

where $\sigma_1$ and $\sigma_3$= major and minor principal stresses, respectively in static triaxial tests. Jenkins et al. (2007) showed that SR is a critical parameter that defines the permanent deformation behaviour of the BSM. As the SR value increases, $\varepsilon_p$ rises. Jenkins et al. (2007)] have discovered that in dynamic triaxial tests carried out using less than 5 x $10^4$ cycles, there is a so-called "Zone of Concern" above SR values higher than an interval ranging between 0.50 and 0.55. In this zone, in equation 1, the N that is needed to reach a specific value of $\varepsilon_p$ is higher than the real one (Figure 3). This causes the acceptance of undesirable materials from a structural point of view. Therefore, it is advisable to conduct dynamic triaxial tests of over 2.5 x $10^5$ cycles, which will allow for the accurate prediction of $\varepsilon_p$ during the fraction of the permanent deformation curve corresponding to Tertiary Flow, i.e., where the relation between $\varepsilon_p$ and N is no longer linear, given that with the increase in N, there is an exponential increment in $\varepsilon_p$. Ebels (2008) fit equation 1 to the results of $\varepsilon_p$ in materials with 25% RAP, observing that the Tertiary Flow began between $10^5$ and $10^6$ load cycles.

4.1.2. *Resilient deformation*

Jenkins et al. (2007) showed that, like unbound granular materials, the predictive equations of the resilient modulus ($M_r$) of the BSM should be obtained by means of dynamic triaxial tests carried out on a wide range of levels of $\sigma_3$ and $\sigma_d$. Ebels (2008) and Santagata et al. (2010) used a simple k-Θ model:

$$M_r = k_1\theta^{k_2} \quad \textbf{(3)}$$

where $\Theta=\sigma_1 + 2\sigma_3$; $k_1$, $k_2$= coefficients. The main drawback of this model is that negative values of Θ, yield incongruent values of $M_r$. Ebels (2008) fit equation 3 to FDR materials containing 25% and 75%

RAP (Table 1). A good fit was had with 25% RAP, whereas the fit was very poor for 75% RAP since $M_r$ depended more on $\sigma_d$ than on $\Theta$. In Italy, Santagata et al. (2010) found reasonable fit for equation 3 in CIR materials with 100% RAP. In Table 1, it can be observed that, for 25% RAP, the addition of 1% of cement produced a rise in $M_r$, since it produces higher parameters $k_1$ and $k_2$. Also, it can be seen that the increase in the RAP percentage from 25% (with 1.0% cement) to 100% (with 2.5% cement) produces a rise in $M_r$, since it produces higher parameters $k_1$ and $k_2$ (Table 1).

On the other hand, Figure 4a shows the variation of $M_r$ as related to $\Theta$ for test temperatures of 20, 40 and 60º C with a short curing time. As the test temperature increased, lower values of $M_r$ were obtained (Santagata et al., 2010). In Figure 4b, it is possible to see the variation of $M_r$ according to $\Theta$ at a fixed temperature of 20º C with three types of curing. As the curing time of the specimens increased, higher values of $M_r$ were obtained. In both figures, for each type of curing or each test temperature, the data are dispersed into vertical strips. According to Santagata et al. (2010), this would seem to indicate that while the behaviour of materials containing 100% RAP is dependent upon $\Theta$, it also depends on their viscoelastic nature.

### 4.2. *Properties of HMA materials*

#### 4.2.1. *Dynamic Modulus*

In the US, several investigators (Thomas & May, 2007; Cross & Jakatimath, 2007; Kim et al., 2009) studied the viscoelastic behaviour of CIR and FDR materials by means of the procedure laid down in the Mechanistic-Empirical Pavement Design Guide (M-E PDG) for HMA. Using this procedure it is possible to obtain complex dynamic modulus of specimens of CIR and FDR materials (at different temperatures and load application times). The Sigmoid Function is used below to fit the Master Curves to a reference temperature (American Association of State Highway and Transportation Officials, 2004):

$$\log\left|E^*\right| = \delta + \frac{\alpha}{1+e^{\beta+\gamma\log f_r}} \quad \textbf{(4)}$$

where $\left|E^*\right|$ = dynamic modulus; $\delta$=minimum value of dynamic modulus; $\delta+\alpha$=maximum value of dynamic modulus; $\beta$, $\gamma$, parameters that describe the shape of the Sigmoid function; and, $f_r$=reduced frequency at the reference temperature. It is common knowledge that the reduced frequency ($f_r$) is related to the test frequency (f) by means of the so-called Shifting Factor $\alpha$(T).

Thomas & May (2007) and May (2008) reported that the M-E PDG considers FDR and CIR materials to be unbound granular materials. This method uses, by default, a dynamic modulus of 138 MPa for FDR materials and a dynamic modulus of 206 MPa for CIR mixtures. In keeping with this, Thomas & May (2007) and May (2008) argued that 138 MPa for FDR materials and 206 MPa for CIR mixtures are not realistic values, since dynamic modulus of 4415 MPa; 3920 MPa; 5565 MPa were obtained in the three FDR materials, respectively, at 21ºC and a frequency of 10 Hz (Table 2). Cross & Jakatimath (2007) obtained dynamic modulus of 2750 MPa in the CIR material at the same temperature and frequency (Table 2).

On the other hand, Figure 5 shows the master curves of these four BSM materials. The remaining types of materials are two conventional HMA with PG 76-28 and PG 70-28 bitumen, respectively. In Figure 5, it is possible to confirm that the viscoelastic behaviour of the FDR materials (25 and 75% RAP without cement) is less pronounced than that of HMA. Accordingly, the master curves of the FDR are more spread out, with a much less pronounced slope. In both low reduced frequencies (milder temperatures) and high reduced frequencies (colder temperatures) the dynamic modulus of the FDR is lower than that of HMA. However, at high temperatures the dynamic modulus of the FDR material with 25% RAP + 1% cement is greater than that of the HMA. Moreover, the master curve of the material having 100% RAP is below that of all the other materials. Therefore, the mixtures containing 25%, 75% and 100% RAP are more prone to permanent deformation (Rutting) and have less tendency to crack under low temperatures (Thermal cracking) than HMA. Nevertheless, the mixture with 25% RAP + 1% cement is the most resistant to permanent deformation. In Figure 5, it can be observed that an increment in RAP content produces a decrease in the dynamic modulus whereas the addition of 1% cement causes it to increase.

4.2.2. *Creep Compliance*

Mamlouk (1984) and Ebels (2008) used Burger's Model (a combination of the Maxwell and the Kelvin model) to evaluate the viscoelastic response of the BSM. This model is composed of three parts: instantaneous elastic, viscous and delayed elastic (Huang, 2004):

$$J(t) = \frac{\varepsilon(t)}{\sigma} = \frac{1}{E_0} + \frac{t}{\lambda_0} + \frac{1}{E_1}\left(1 - e^{-\frac{E_1 t}{\lambda_1}}\right) \quad \textbf{(5)}$$

where J(t)= creep compliance in time t; σ= stress applied; ε(t)= strain in time t; $E_0$ and $\lambda_0$ = elasticity and viscosity modulus, respectively, in the Maxwell Model; $E_1$ and $\lambda_1$ = elasticity and viscosity modulus, respectively, in the Kelvin Model. It is well know that under a constant stress the creep compliance is the reciprocal of Young´s modulus (Huang, 2004). Mamlouk (1984) conducted creep tests on a material designed with 60% RAP (3.5 % residual bitumen). Also, Ebels (2008) obtained the parameters of equation 5 on the FDR materials described in Table 1. Mamlouk (1984) and Ebels (2008) observed that, in general, the values of the parameters of equation 5 decreased as the test temperature increased resulting in softer mixtures whereas these values rose with increasing curing times resulting in stiffer mixtures. Also, Ebels (2008) observed that an increase in RAP content resulted in decreasing parameter values of Burger's Model (Table 3) As a result, the increase of RAP from 25 to 75% produced a slight increase of J(t) at various times (Figure 6). Thus, the mix with 25% RAP is slightly stiffer than the mixture with 75% RAP. Nevertheless, with 25% RAP, the addition of 1% cement caused the parameters to increase (Table 3), thus J(t) at various times decreased. This can be observed in Figure 6 where with 25% RAP + 1 cement the J(t) values at various times are lowest, therefore this mixture is stiffer than the one with 25% RAP.

**Comentario [MS2]:** "en el tiempo"

**Comentario [MS3]:** "Mezclas más rígidas" o "stiffener" mezclas que refuerzan ¿?

4.2.3. *Resilient Modulus*

Some investigators have preferred to use the indirect tensile stiffness modulus test (ITSM) to characterize the stiffness of BSM. The resilient modulus is obtained by means of repeated load tests carried out under diametrical compression, with the total recoverable deformation being recorded throughout the load cycle. The following formula is used to calculate the resilient modulus (RM) (MPa) (Huang, 2004):

$$RM = \frac{P(\mu + 0.27)}{h \cdot \delta_h} \quad \textbf{(6)}$$

where P= maximum applied repeated load: μ= Poisson coefficient; h= specimen thickness (mm); $\delta_h$=total horizontal recoverable deformation (mm). In Portugal, Batista & Antunes (2003) found that the RM of CIR materials (without cement) decreased as the test temperatures rose. Sunarjono (2007)

also observed that in tests carried out at temperatures of 20ºC, the RM of CIR materials (without cement) increased as the specimen curing time increased, whereas they decreased with higher moisture content. Zulakmal et al. (2009) conducted RM tests on specimens made with 0, 25, 50, 75 and 100% RAP. These investigators used different percentages of cement and moisture as well as different specimen curing times. In keeping with this, they observed that the RM increased with both increasing curing times and increased percentages of cement. The RM decreased as the percentage of RAP rose. The highest RM were obtained using specimens made with a low percentage of RAP and a low percentage of moisture. Yan et al. (2010) reported that when a constant temperature is maintained in CIR materials (with 3.5% emulsion and 1.5% cement), the RM decreases as the stress level increases, whereas for the same stress level, the RM decreases as the temperature increases. Kavussi & Modarres (2010a; 2010b) and Modarres et al. (2011) fit exponential and logarithmic functions to study the variation in the RM (CIR materials with cement) (Figure 7). A curing time of 120 days, 4% emulsion and 1% cement content at a test temperature of 20ºC yielded a RM of 3000 MPa. In Figure 7, it is possible to see that the RM increases as the test temperature decreases, with increasing curing times and an increase in the percentage of cement. According to these investigators, there is a greater increase in stiffness due to the drop in test temperature rather than because of increased curing times (Figure 7).

4.2.4. *Fatigue resistance*

Some researches have investigated the fatigue resistance of BSM by means of several fatigue tests carried out in the laboratory. According to Kavussi & Modarres (2010a) the fatigue resistance of BSM with 100% RAP is similar to that of open-graded HMA. In order to examine this resistance, several investigators have fit equation 7 to the experimental data from the fatigue tests conducted in the lab (Ebels, 2008; Batista & Antunes, 2003; Miró et al. 2004):

$$N_f = f_1(\varepsilon_t)^{-f_2} \quad (7)$$

where $N_f$ =number of load cycles until fatigue failure occurs; $\varepsilon_t$=maximum tensile strain; $f_1$, $f_2$,=coefficients. In Portugal, Batista & Antunes (2003) carried out indirect tensile fatigue tests (ITFT) on cylindrical specimens at a temperature of 20ºC. These investigators observed that the fatigue lines

of CIR materials were similar to the line of the reference HMA. In Spain, Miró et al. (2004) carried out dynamic flexotraction fatigue tests (three point beam at 10 Hz and 20ºC) on CIR and HMA cores. The fatigue laws of CIR materials had a greater slope than those of HMA. For the same $\varepsilon_t$, the fatigue life $N_f$ was lower in the CIR materials. Ebels (2008) also performed dynamic flexotraction tests (four point beam at 10 Hz and 5ºC). In this case as well, $N_f$ was found to be lower in the FDR materials described in Table 1. However, Ebels (2008) stated that, since FDR materials have a lower stiffness than HMA, fatigue failure should not be used as the main criterion for its design. Ebels (2008) observed that both an increase in the percentage of RAP and the addition of 1% cement resulted in a decrease in $N_f$.

In Iran, Kavussi & Modarres (2010a) and Modarres et al. (2011) carried out indirect tensile fatigue tests (ITFT) on cylindrical specimens of CIR materials with cement. These investigators found that when high initial strains were imposed, the stiffness increased and the fatigue slope lines decreased when the percentage of cement increased as well as when the test temperature decreased (Figure 8). However, an increase in the curing time of the specimens made with cement did not have such an effect on the fatigue slope lines. The relationship between resilient modulus and fatigue life was determined by Kavussi & Modarres (2010a) who calibrated two fatigue models for values of strain ($\varepsilon$) less than or greater than 300 μm/m:

$$\begin{aligned} N_f &= a\, e^{b\varepsilon}\, (RM)^c && \varepsilon < 300\ \mu m/m \\ N_f &= a\, e^{b\varepsilon + cRM} && \varepsilon > 300\ \mu m/m \end{aligned} \qquad \textbf{(8)}$$

where a, b and c= coefficients. These investigators found that for $\varepsilon$ <300 μm/m, $N_f$ increased as resilient modulus rose, while for $\varepsilon$ >300 μm/m, the opposite occurred (Figure 9). Consequently, for pavements with heavy loading conditions, the increase in the percentage of cement has a negative effect on the fatigue life of CIR materials. Lastly, Santagata et al. (2009) conducted the same type of test on CIR materials with cement, and they discovered that for a constant percentage of cement, the specimens having the highest percentage of emulsion showed greater fatigue resistance.

## 5. Final remarks

### 5.1. *Behaviour phases of BSM*

As discussed in section 3, based on the research conducted on a real scale, it was seen that the behaviour of BSM consists of two phases: the Curing Phase and the Stiffness Reduction Phase. However this two-phase hypothesis is rather simplistic since we are dealing with a type of material (FDR or CIR) that is essentially in evolution from a mechanical point of view. For this reason, we have made a four-stage proposal determined from in-place observations of BSM works in Spain:

I. Initially the material virtually lacks cohesion ($c$) and the internal friction ($\phi$) is negatively affected by the presence of water.

II. In stage II, the growth of $c$ is still not very significant, but the incidence of water in $\phi$ is negligible, which means that the behaviour may be compared to that of unbound granular materials.

III. Next the material enters into a stage in which $c$ is significant although the expected maximum value has not been reached and, as is logical, resistance is also a concern owing to $\phi$.

IV. Once the maximum cohesion has been attained, the material is theoretically similar to a HMA, but with a different type of behaviour, not only because of the value of the stiffness modulus under certain conditions of temperature and load application speed, but also because of its clearly different response to these variables as well as its relation to the process of damage accumulation.

Stages I, II and III belong to the Curing Phase and subsequent to stage IV when the Stiffness Reduction Phase begins. The intrinsic characteristic of these materials is the presence of water and, as a result, the immediate procurement of the desired cohesion is not attained. In most cases, stage I would last for a very short time, possibly a question of hours. Therefore, the Curing Phase would be virtually reduced to stages II and III, which could last for months and in some cases, in very damp climates, for years. Because of the difficulty entailed, the behaviour hypotheses studied in section 4.1 do not take into account the evolution of the behaviour of the material during these two stages during which the curing process is carried out. This is especially true in FDR materials with a lower percentage of RAP, where the materials exhibit a more highly variable behaviour, which therefore makes prediction more difficult. Lastly, in stage IV, when the BSM have reached the maximum

cohesion, it behaves similar to a HMA, which means that theoretically equations 1 to 3 are not appropriate and that equations 4 and 5 should be used.

**5.2.** ***Reproduction of the behaviour phases in the lab***

In keeping with this, a very important aspect, which is an obstacle to the investigation of these materials, is the fact that it is difficult to obtain an accurate laboratory reproduction of the degree of evolution of curing during stages II and III. In stage IV the specimens representing this degree of the material's evolution must be completely cured in the lab. This question is important when conducting the mechanical tests that will be used to determine the mechanical properties (equations 1 to 5). In the references listed in this article there are many different curing procedures. They all try to reproduce the specific conditions of the materials, ambient temperature, compaction energy, moisture, etc., in their countries of origin, which probably indicates that none of them are sufficiently good.

**5.3.** ***Failure criterion***

The increase in stiffness of the BSM during the first period after construction would indicate that the deterioration due to fatigue (and the loss of stiffness associated with it), does not occur during the first phase of the service life of the pavement (or it is eclipsed by the effect of curing). This would imply that another failure mechanism is at work here, in this case, shear stress failure will be the failure criterion.

However, once maximum cohesion has been reached BSM become dependent upon the load application time and temperature, and theoretically, they tend to behave like HMA. As has been discussed in section 4.2, in comparison with HMA materials, BSM have a reduced flexural stiffness. Their behaviour is more elastic and less viscous; their fatigue laws, however, are apparently less favourable. In keeping with this, it is important to remember that most of the materials described in sections 4.2.3 and 4.2.4 were made with cement, which causes fatigue resistance to diminish. It is common knowledge that cracking due to fatigue is one of the main failure mechanisms of HMA materials. So, the question is, do BSM fail because of cracking due to fatigue? Clearly, more research is needed on this subject. It may be that the fatigue tests used (four point flexural beam, indirect tensile fatigue tests, etc.) are not appropriate to evaluate the fatigue behaviour of BSM.

According to Ebels (2008), BSM exhibit properties that can be related to flexural fatigue. However, Collings & Jenkins (2011) consider that the non-continuously bound nature of BSM, together with their relatively low stiffness, does not create conditions that are favourable for the formation and propagation of conventional fatigue cracks, since tensile stress concentration at a crack-head can simply not develop within a material that is not continuously bound. In France, Goacolou et al. (1997) did not observe the same failure mechanisms due to flexural fatigue in bituminous materials made with emulsion. Based on the results of the Accelerated Pavement Testing (APT) performed on the pavement test track in the lab of the LCPC (Pavement Fatigue Carrousel) Goacolou et al. (1997) found that cracking due to the fatigue of materials with emulsion occurs on a different scale. Micro-cracking, at close intervals, appears in materials with emulsion, whereas macro-cracking, located at greater distances from each other, takes place in HMA materials. This is because materials with emulsion (particularly those having a low RAP content) have a lower degree of cohesion and their behaviour bears a greater resemblance to that of unbound granular materials. Under these conditions, the mechanism through which the finer cracks are propagated to the upper layer may not be the same as that of the larger cracks found in HMA materials.

### 5.4. *Technological gaps*

It's evident that the knowledge of the mechanical properties and behaviour of BSM have some technological gaps. It's feasible to fill these technological gaps but requires a great deal of research. A starting point can be the four stages proposed in section 5.1. However, it is necessary to investigate the relation between the LTPP data of in-service pavements made with BSM and their mechanical properties and behavioural models obtained in the laboratory. Also, the evolution of moisture of BSM layers in relation to the curing time during the first phase in stages II and III should be investigated, as well as, the evolution of the stiffness after some time and traffic during stages II and III (stiffness increase) and during stage III (stiffness decrease). The laboratory mechanical test protocols must reproduce the degree of evolution of moisture with relation to the curing time. Finally, BSM samples must be classified into categories. Each category should indicate a specific type of BSM with the same range of properties.

**Comentario [MS4]:** "con el (paso del) tiempo"

## 6. Conclusions

The critical review of the behaviour of BSM has led to the following conclusions:

- In any event, it is clear that during the service life of BSM there are at least two phases: The first phase marks an increase in the initial stiffness owing to the curing and densification of the material. During this phase, the BSM are considered to behave like an unbound granular material with stress dependency. During the second phase of the material, stiffness is reduced. In this second phase the BSM are considered to behave like a viscoelastic material, but it is less dependent on temperature and load frequency than HMA materials.
- When BSM are considered to be similar in form to unbound granular materials, the most important property is resistance to permanent deformation, which depends on shear stress ($c$ and $\phi$) as well as on the ratio between the deviator stress and the deviator stress at failure (Stress Ratio). Another important parameter is the resilient modulus ($M_r$) obtained in dynamic triaxial tests, which increases with the addition of cement and an increment in curing time.
- When BSM are considered to be similar in form to HMA, the viscoelastic properties are analyzed by means of the dynamic modulus and Creep compliance. In the US, there is a certain tendency to characterize this behaviour by means of master curves. In general terms, BSM exhibit a lower flexural stiffness than HMA. This dynamic modulus increases as the percentage of RAP diminishes. It also increases with the addition of cement and an increment in curing time. Other researchers prefer to use the resilient modulus (RM) obtained with the indirect tensile stiffness modulus test, which tends to decrease as the percentage of RAP augments. Lastly, BSM exhibit properties that may be related to cracking due to flexural fatigue. This cracking, however, seems to occur on a different scale to that of HMA materials.
- The structural design of BSM based on more in-depth knowledge of their mechanical behaviour and structural properties is a field of investigation that still needs to be developed, as technical and scientific information is still relatively scarce. The reasons for this fact are the complexity to obtain an accurate laboratory reproduction of the degree of evolution of curing and the difficulty

to develop a design method to take account of the evolution in BSM stiffness after some time time.

**Acknowledgements**

The authors are grateful to the Ministry of Science and Innovation of the Spanish government for providing the financial support for this research paper within the framework of the FÉNIX Research Project (Strategic investigation for safer and more sustainable roads), subsidized by the program CENIT 2007 of the Centro para el Desarrollo Tecnológico e Industrial (CDTI).

**References**

American Association of State Highway and Transportation Officials (AASHTO). (2004). *Development of the 2002 Guide for the Design of New and Rehabilitation Pavement Structures*. Design Guide and Supplemental Documentation, NCHRP Project 1-37A, Transportation Research Board of the National Academies, Washington, D.C.

Asphalt Academy. (2009). *Technical Guideline: Bitumen Stabilised Materials. A Guideline for the Design and Construction of Bitumen Emulsion and Foamed Bitumen Stabilised Materials*. TG 2 Second edition, South Africa.

Batista, F. & Antunes, M. (2003). *Pavement rehabilitation using asphalt cold mixtures*. Proceedings of the 3rd International Symposium Maintenance and Rehabilitation of Pavements and Technological Control. University of Minho, Guimaraes, Portugal, pp. 653-662.

Collings, D., & Jenkins, K. (2011). The long-term behaviour of Bitumen Stabilised Materials (BSMs). 10th Conference on Aspahlt Pavements for South Africa.

Cross, S.A., & Jakatimath, Y. (2007). *Evaluation of Cold In-Place Recycling for Rehabilitation of Transverse Cracking on US 412*. Final Report. The Oklahoma Department of Transportation.

del Val, M.A., & Rocci, S. (1998) Guía para el dimensionamiento de firmes reciclados en frío, Probisa, Spain.

Ebels, L. J. (2008). *Characterisation of Material Properties and Behaviour of Cold Bituminous Mixtures for Road Pavements*. Dissertation presented for degree of Doctor of Philosophy (Engineering). Stellenbosch University, South Africa.

Goacolou, H., Bourlot, F., Borosseaud, Y., Gramsammer, J-C., & Kerzreho, J-P. (1997). Expérimentation (deusxième partie) de la Grave-Mousse sure le manège de fatigue. *Revue Gènerale des Routes et des Aerodromes*, 754, 73-78.

Huang, Y.H. (2004). *Pavement Analysis and Design*. Second ed., PersonPrentice Hall.

Jenkins, K.H., Long, F.M., & Ebels, L.J. (2007). Foamed bitumen mixes=shear performance? *International Journal of Pavement Engineering*, 8, 85-98.

Jenkins, K.H., & Yu, M. (2009). *Cold-Recycling Techniques Using Bitumen Stabilization: Where is This Technology Going?* ASCE Geotechnical Special Publication 191, p. 191-200.

Kavussi, A., & Modarres, A. (2010a). Laboratory fatigue models for recycled mixes with bitumen emulsion and cement. *Construction and Building Materials*, 24, 1920-1927.

Kavussi, A., & Modarres A. (2010b). A model for resilient modulus determination of recycled mixes with bitumen emulsion and cement from ITS testing results. *Construction and Building Materials*, 24, 2252-2259.

Kim, Y., Lee, H.D., & Heiztman, M. (2009). Dynamic Modulus and Repeated Load Tests of Cold In-Place Recycling Mixtures Using Foamed Asphalt. *Journal of Materials in Civil Engineering*, 21, 279-285.

Kumar, C.K., Kumar, D.S.N.V.A., Reddy, M.A., & Reddy, K.S. (2008). Investigation of cold-in place recycled mixes in India. *International Journal of Pavement Engineering*, 9, 265-274.

Liebenberg, J.J.E., & Visser, A.T. (2003). Stabilization and Structural Design of marginal Materials for Use in Low-Volume Roads, *Transportation Research Record*, 1819, 166-172.

Liebenberg, J.J.E., & Visser, A.T. (2004). Towards a mechanistic structural design procedure for emulsion-treated base layers. *Journal of South Africa Institution of Civil Engineers*, 46, 2-8.

Loizos, V., & Papavasiliou, V. (2006). Evaluation of Foamed Asphalt Cold In-Place Pavement Recycling Using Non-destructive Techniques. *Journal of Transportation Engineering*-ASCE, 132, 970-988.

Manlouk, M.S. (1984). Rheology of Cold-recycled Pavement Materials Using Creep Test. *Journal of Testing Evaluation*, 12, 341-347.

May, R.W. (2008). The Challenges to innovation with the M-E PDG-Case Study: Cold Recycled Mixtures (With Discussion). *Journal of the Association of Asphalt Paving Technology*, 77, 985-1004.

Miró, R., Martínez, A., & Güel, A. (2004). *Case Study of Cold In-Place Recycled Asphalt Pavement of the N-536 Highway in Spain*. Proceedings of Transportation Research Board 83$^{th}$ Annual Meeting (CD-ROM), Transportation Research Board, Washington, D.C.

Modarres, F.M., Nejad, A., Kavussi, A., Hassani, E., & Shabanzadeh, E. (2011). A parametric study on the laboratory fatigue characteristics of recycled mixes. *Construction and Building Materials*, 25, 2085-2093.

Santagata, F.A., Bocci, M., Grilli, A., Cardone, F. (2009). *Rehabilitation of an Italian highway by Cold In-Place Recycling techniques*. Advanced Testing and Characterization of Bitumen Materials, Taylor & Francis Group (Eds.), p. 1113-1122.

Santagata, E., Chiappipinelli, G., Riviera, P.P., & Baglieri, O. (2010). Triaxial Testing for the Short Term Evaluation of Cold-Recycled Bituminous. *Road Materials and Pavement Design*, 11, 123-147.

Sunarjono, S. (2007). Tensile strength and stiffness modulus of foamed asphalt applied to a grading representative of Indonesian road recycled pavement materials. *Dinamika TEKNIK SIPIL*, 7, 1-10.

Theyse, H.L., de Beer, M., & Rust, F.C. (1996). *Overview of the South African Mechanistic Pavement Design Analysis Method*. Proceedings of Transportation Research Board 75th Annual Meeting (CD-ROM), Transportation Research Board, Washington, D.C.

Thomas, T.W., & May, R. W. (2007). *Mechanistic-Empirical Design Guide Modelling of Asphalt Emulsion Full Depth Reclamation Mixes*. Proceedings of Transportation Research Board 86th Annual Meeting (CD-ROM), Transportation Research Board, Washington, D.C.

Yan, J., Ni, F., Yang, M., & Li, J. (2010). An experimental study on fatigue properties of emulsion and foam cold recycled mixes, *Construction and Building Materials*, 24, 2151-2156.

Zulakmal, S., Nfisah, A.A., Mohd, M., & Mat, H. (2009). I*nfluence of active filler, curing time, and moisture content on the strength properties of emulsion and foamed bitumen stabilized mix*. Advanced Testing and Characterization of Bitumen Materials, Taylor & Francis Group (Eds), p. 1143-1150.

Table 1. Characteristics of four BSM.

| Characteristic | FDR* | | | CIR- | |
|---|---|---|---|---|---|
| | 25% RAP | 75% RAP | 25% RAP + 1 cement | 100% RAP | |
| Gradation | Dense mix | | | Dense mix | |
| Maximum aggregate size (mm) | 19 | | | 20 | |
| Emulsion type | Cationic: 65% asphalt, 35% water | | | Cationic: 60% asphalt, 40% water | |
| Emulsion content (%) | 5.5 | 3.7 | 5.5 | 3.5 | |
| Added water content (%) | 5.7 | 3.9 | 5.7 | 2.5 | |
| Active cement filler | NO | NO | 1.0% cement | 2.5% cement | |
| Virgin aggregate | Limestone | | | NO | |
| Compaction | Superpave Gyrator Compactor 30 gyrations | | | | |
| Curing | 20 hours at 30ºC+20 hours 40ºC (sealed)+24 hours at 40ºC | | | 18 to 24 hours at 20ºC + 1 to 2.5 hours at 20ºC | 18 to 24 hours at 20ºC + 7 days at 20 ºC | 18 to 24 hours at 20ºC + 6 days at 40ºC + 1 day at 20ºC |
| Air Voids (%) | N/A | N/A | N/A | 12.2 | |
| Sample dimensions | 260 mm height, 150 mm diameter | | | 200 mm height, 100 mm diameter | |
| c (KPa) range | 142 to152 | 195 to 206 | 387 to 390 | N/A | |
| ϕ (º) range | 38.4- to 43.7 | 29.7 to 33.8 | 33.8 to 32.2 | N/A | |
| Parameters k-Θ model (k1/k2) | 130 (MPa)/0.30 | N/A | 150 (MPa)/0.33 | 715(MPa)/0.49 | 898 (MPa)/0.45 | 998 (MPa)/0.47 |

Note: * Ebels (2008): FDR -25% RAP; FRD -75% RAP and FDR -25% RAP +1% cement (CEM );
+ Santagata et al. (2010):CIR -100% RAP
N/A=No research data available

Table 2. Characteristics of four BSM.

| | FDR* | | | CIR+ |
|---|---|---|---|---|
| Characteristic | 25% RAP | 75% RAP | 25% RAP + 1 cement | 100% RAP |
| Gradation | Dense mix | | | |
| Maximum aggregate size (mm) | 20 | | | 19 |
| Emulsion type | Cationic: 65% asphalt, 35% water | | | |
| Emulsion content (%) | 5.5 | 3.5 | 5.5 | 3.0 |
| Added water content (%) | 4.9 | 3.0 | 4.9 | 2.0 |
| Active cement filler (%) | NO | NO | 1.0 | NO |
| Virgin aggregate | Limestone | | | NO |
| Compaction | Superpave Gyrator Compactor 30 gyrations | | | Superpave Gyrator Compactor 30-40 gyrations |
| Curing | 72 hours at 40º C | | | 48 hours at 60º C |
| Air Voids (%) | 15.5 | 14.0 | 14.2 | 12.0 |
| Sample dimensions | 150 mm height, 100 mm diameter | | | |
| Dynamic Modulus (MPa) (21.1ºC; 10 Hz) | 4415 | 3920 | 5565 | 2750 |
| Test protocol | AASHTO TP-62 | | | |

Note: * Thomas & May (2007): FDR -25% RAP; FRD -75% RAP and FDR -25% RAP +1% cement (CEM );
+ Cros & Jakatimath (2007):CIR -100% RAP

Table 3. Burges model parameters at 20ºC of three FDR materials at 20ºC (Ebels, 2008).

| Parameter | 25% RAP | 75% RAP | 25% RAP + 1 cement |
|---|---|---|---|
| $E_0$ (MPa) | 2342 | 1809 | 2665 |
| $E_1$ (MPa) | 2911 | 2912 | 5324 |
| $\lambda_0$ (MPa s) | 640 | 562 | 1291 |
| $\lambda_1$ (MPa s) | 161 | 258 | 123 |

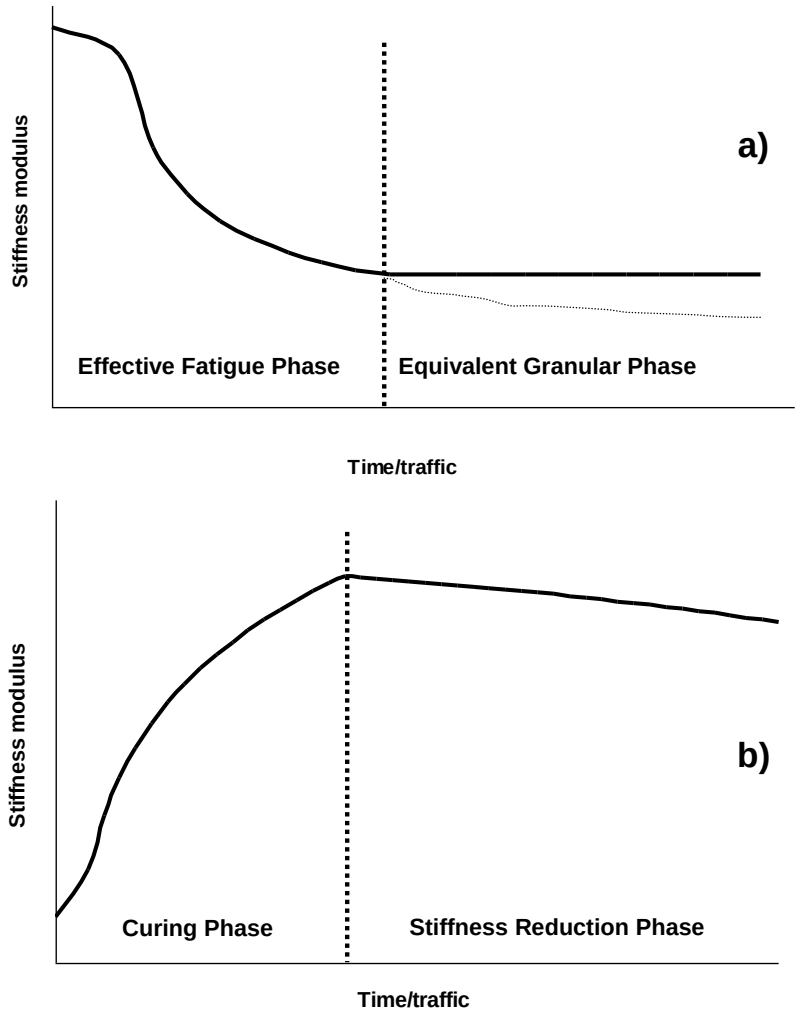


Figure 1. Hypothesis of the behaviour of BSM: a) Effective Fatigue Phase-Equivalent Granular Phase b) Curing Phase-Stiffness Reduction Phase

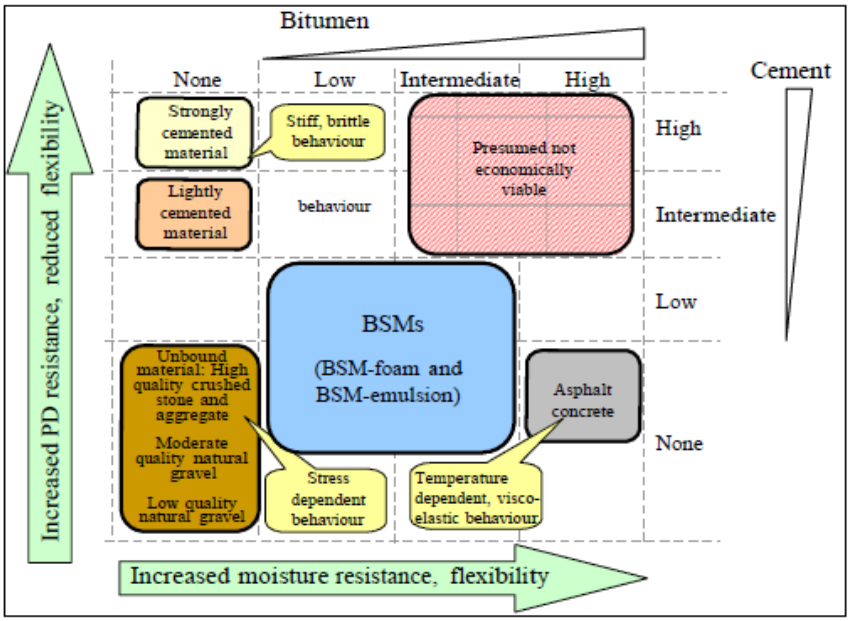


Figure 2. Matrix of bituminous and mineral binder influence on BSM behaviour (Asphalt Academy, 2009)

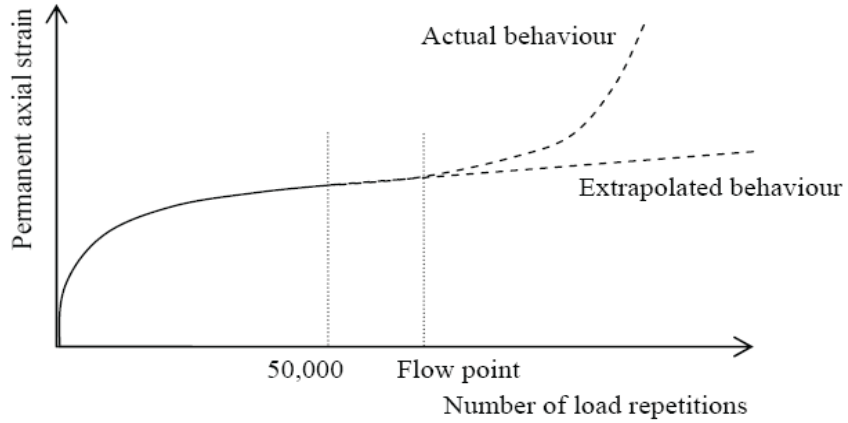


Figure 3. Actual and extrapolated behaviour due to triaxial dynamic test carried out using less than 5 x $10^4$ cycles (Ebels, 2008)

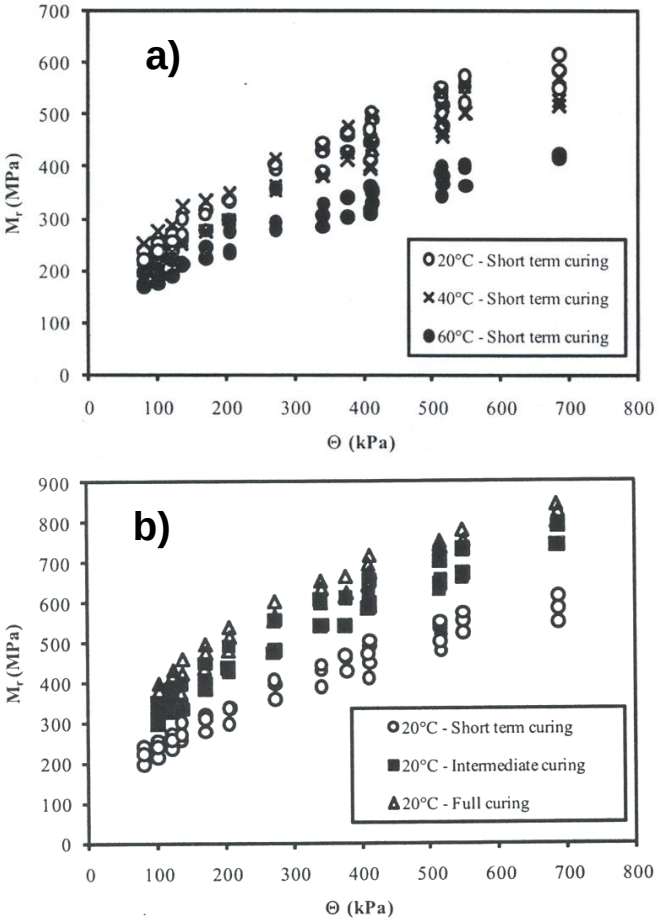


Figure 4. $M_r$ versus Θ of a CIR material: a) 20, 40 and 60ºC, short-term curing b) 20ºC, three curing times (Santagata et al., 2010).

Note: Short=conditioning from 18 to 24 hours at temperatures of 20, 40 or 60ºC + curing time of 1 to 2.5 hours at 20, 40 or 60 ºC; intermediate=conditioning of 18 to 24 hours at 20ºC + curing time of 7 days at 20 ºC; full=conditioning from 18 to 24 hours at 20ºC + curing time of 6 days at 40 ºC + 1 day at 20ºC

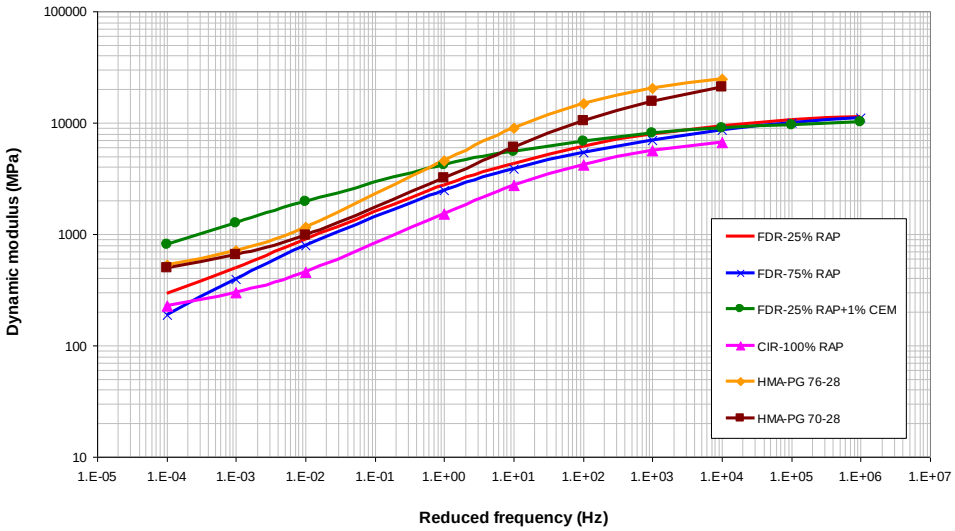


Figure 5. Master curves of six bituminous materials.

Note: The master curves were drawn using the parameters of the following technical references:

- Thomas & May (2007): FDR -25% RAP; FRD -75% RAP and FDR -25% RAP +1% cement (CEM )
- Cros & Jakatimath (2007):CIR -100% RAP, HMA -PG 76-28 and HMA -PG 70-28

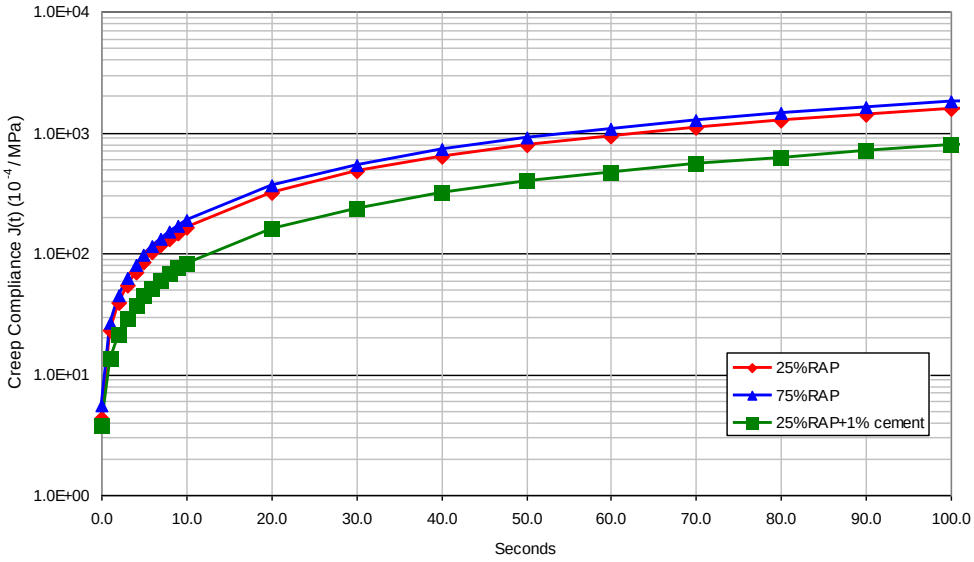


Figure 6. Creep compliance curves in time of three FDR materials at 20ºC.

Note: The Creep Compliance curves were drawn using parameters of Table 3.

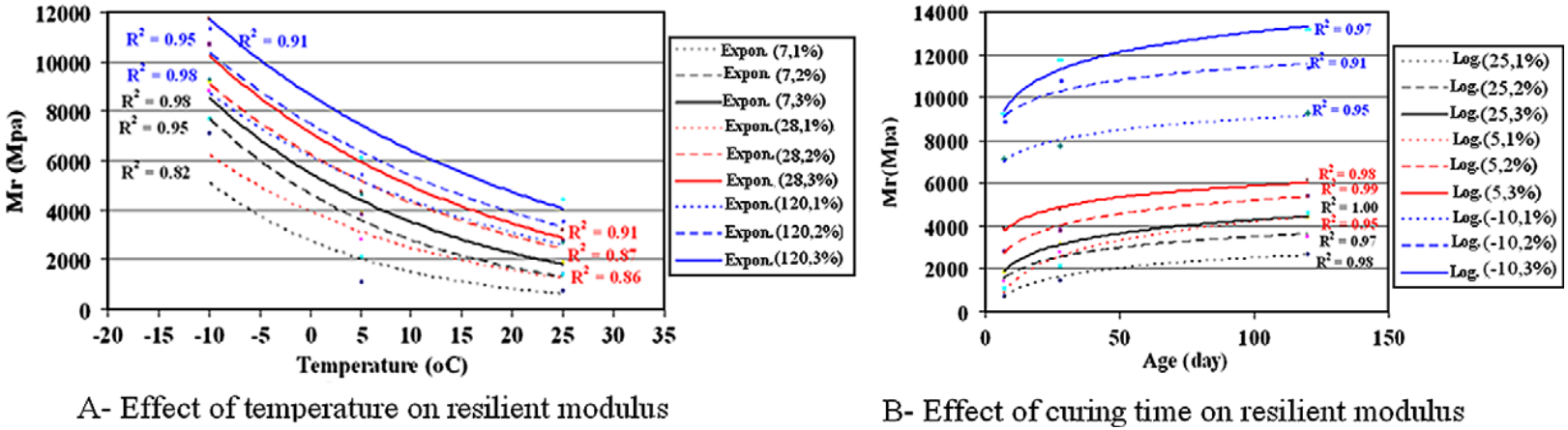


Figure 7. Effect of temperature and curing time on the Resilient modulus of CIR materials (Kavussi & Modarres, 2010).

Note: A. In the legend the first and second number correspond to the curing time in days and % of cement respectively.
B. In the legend the first and second number correspond to the test temperature in °C and % of cement respectively.

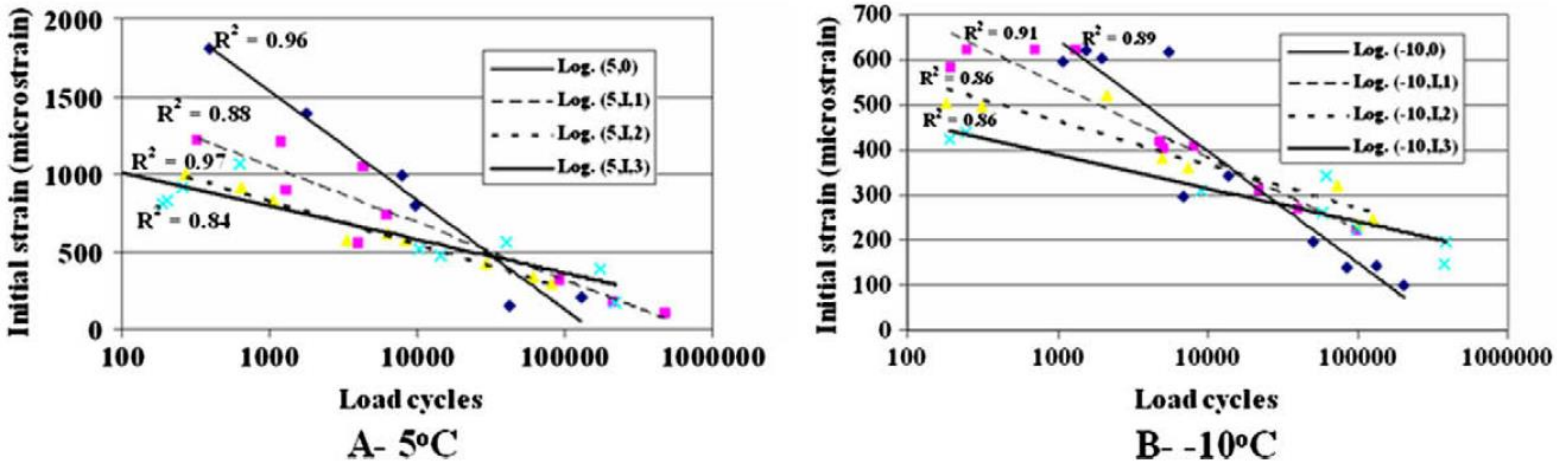


Figure 8. Fatigue lines of CIR materials (Kavussi & Modarres, 2010).

Note: In the legend the first and second number correspond to the test temperature in ºC and % of cement respectively.

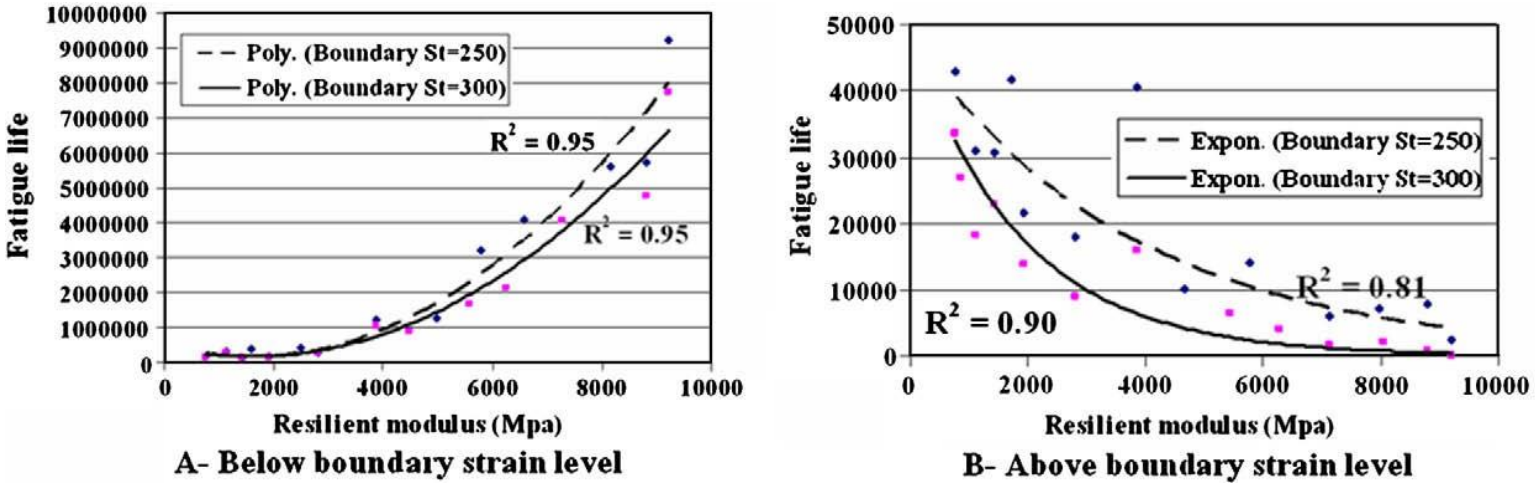


Figure 9. Fatigue life – MR relationship considering 250 and 300 microstrain as boundary strain levels of CIR materials (Kavussi & Modarres, 2010).